NOMA-based Compressive Random Access using Gaussian Spreading

Jinho Choi

Abstract—**Compressive random access (CRA) is a random access scheme that has been considered for massive machine-type communication (MTC) with non-orthogonal spreading sequences, where the notion of compressive sensing (CS) is used for low-complexity detectors by exploiting the sparse device activity. In this paper, we study the application of power-domain non-orthogonal multiple access (NOMA) to CRA in order to improve the performance of CRA (or increase the number of devices to be supported). We consider Gaussian spreading sequences and derive design criteria through a large-system analysis to determine the power levels for power-domain NOMA. From simulation results, we can confirm that the number of incorrectly detected device activity can be reduced by applying NOMA to CRA.**

Index Terms—**Gaussian spreading; Multiuser Detection; Random Access; Machine-Type Communications (MTC)**

I. Introduction

Machine-type communication (MTC) becomes a key element for the Internet of Things (IoT) as it is to support massive IoT connectivity in 5th generation (5G) networks [1] [2] [3]. There are also existing standards for MTC in Long-Term Evolution (LTE) networks [4] [5] [6]. Although there are a large number of devices, since only a few are active at a time, it is preferable to use an uncoordinated transmission scheme such as a random access scheme. Thus, most MTC schemes are based on random access. In particular, ALOHA [7] is mainly considered for MTC [8] [9] [10] [11].

In order to exploit the sparse activity of devices in massive MTC, the notion of compressive sensing (CS) [12] [13] can be exploited for random access, where the resulting scheme is referred to as compressive random access (CRA) [14]. CRA can also be seen as the application of code division multiple access (CDMA) to random access, where the user activity detection and data detection are carried out using CS algorithms [15] [16] [17]. The main advantage of CRA over conventional multichannel random access schemes (e.g., multichannel ALOHA) is that it uses non-orthogonal spreading sequences to effectively increase the number of multiple access channels, while low-complexity CS-based detectors can be used for the user activity detection [18].

Existing CRA schemes can be divided into two groups. One group is based on handshaking process (e.g., the random access channel (RACH) procedure in [5]) and the other group is based on grant-free transmission. When CRA is used in handshaking process, a CS algorithm is used to detect the preambles that are transmitted by active devices. In grant-free transmission, each user is to have a unique spreading code

and CRA is used to detect the signals from active users. For example, in [19], CRA is used for the RACH procedure where joint channel estimation and preamble detection is carried out. In [14] [20] [21] [22] [23], CRA is used for grant-free transmission. In particular, in [14] [20] [21], joint channel estimation and data detection for CRA under a frequency-selective fading environment is considered. In [22] [23], advanced CS algorithms are considered for the signal detection. Furthermore, in [24], in order to support a large number of devices with grant-free CRA, coded sparse identification vectors are studied in conjunction with joint data detection and device identification.

As explained in [23], grant-free CRA can take advantage of multiple measurement vector (MMV) setup [25] [26], which also allows to derive performance limits of CRA as in [18], while its performance mainly depends on the length of spreading codes, the number of devices, the sparsity, and the background noise. In general, the ratio of the length of spreading codes to the number of devices is a key parameter that determines the number of the active devices that can be successfully detected. Thus, in order to improve the performance, a longer length of spreading codes or a wider system bandwidth is required.

To improve the spectral efficiency, non-orthogonal multiple access (NOMA) has been extensively studied for cellular systems [27] [28] [29] [30]. In particular, power-domain NOMA with successive interference cancellation (SIC) is considered to support multiple users with the same radio resource block. The notion of NOMA can be employed for random access as in [31] [32], which results in a higher throughput.

In this paper, we apply power-domain NOMA to CRA in order to improve the performance of CRA for a given length of spreading codes or a system bandwidth with multiple layers in the power domain. This approach differs from that in [32] as the spreading codes in this paper are not orthogonal. While the application of NOMA to CRA is straightforward, it is necessary to carefully determine the power levels for successful SIC with a high probability. To this end, we consider Gaussian spreading (i.e., Gaussian vectors for spreading codes), which results in a Gaussian-like interference due to the signals in the other layers. With Gaussian spreading, we can derive design criteria through a large-system analysis to determine the power levels for successful SIC through multiple layers as in the power-domain NOMA when the maximum a posteriori probability (MAP) detection is employed. Provided that SIC can be successfully carried out, the throughput of CRA can be improved by a factor of the number of layers. However, due to the transmit power limitation and the error propagation (in SIC), the number of layers might be limited.

The author is with the School of Information Technology, Deakin University, Burwood, VIC 3125, Australia (e-mail: jinho.choi@deakin.edu.au)

The main contributions of the paper are as follows: *i)* a novel CRA scheme based on NOMA is proposed to improve the performance; *ii)* design criteria are derived with Gaussian spreading for successful SIC with a high probability; *iii)* a low-complexity detection method (to find an approximate solution to the MAP detection) is proposed for the device activity detection.

The rest of the paper is organized as follows. In Section II, we present the system model for CRA. We apply NOMA to CRA in Section III and discuss SIC. Design criteria are derived through a large-system analysis using Gaussian approximation in Section IV. To find an approximate solution to the MAP detection problem with low-complexity, we derive an approach based on variational inference in Section V. In Section VI, simulation results are presented. We conclude the paper with some remarks in Section VII.

Notation: Matrices and vectors are denoted by upper- and lower-case boldface letters, respectively. The superscripts T and H denote the transpose and complex conjugate, respectively. The p-norm of a vector $\mathbf{a}$ is denoted by $||\mathbf{a}||_p$ (If $p = 2$, the norm is denoted by $||\mathbf{a}||$ without the subscript). For a vector $\mathbf{a}$, $\mathrm{diag}(\mathbf{a})$ is the diagonal matrix with the diagonal elements from $\mathbf{a}$. For a matrix $\mathbf{X}$ (a vector $\mathbf{a}$), $[\mathbf{X}]_n$ ($[\mathbf{a}]_n$) represents the nth column (element, resp.). $\mathbb{E}[\cdot]$ and $\mathrm{Var}(\cdot)$ denote the statistical expectation and variance, respectively. $\mathcal{CN}(\mathbf{a}, \mathbf{R})$ ($\mathcal{N}(\mathbf{a}, \mathbf{R})$) represents the distribution of circularly symmetric complex Gaussian (CSCG) (resp., real-valued Gaussian) random vectors with mean vector $\mathbf{a}$ and covariance matrix $\mathbf{R}$.

II. SYSTEM MODEL

In this section, we present the system model for grant-free CRA to support MTC.

Suppose that there are K devices and a base station (BS) in a cell. We assume that if device k has a packet at a slot, it becomes active and transmits the packet during the slot. Denote by $x_{k,(t)} \in \mathcal{X}$ the tth symbol of the data packet transmitted from device k to the BS, where $\mathcal{X}$ is the signal constellation. For convenience, we assume that the length of slot is equivalent to the length of packet and a slot consists of T symbol intervals. Like CDMA [33] [34], $\mathbf{g}_k x_{k,(t)}$ is transmitted during a symbol interval, where $\mathbf{g}_k = [g_{1,k} \ \cdots \ g_{N,k}]^{\mathrm{T}}$ is the spreading or signature code of device k. Here, N is referred to as the spreading gain. In general, the system bandwidth is proportional to N when the time duration of slot is fixed. At the BS, the received signal is given by

$$\mathbf{y}_{(t)} = \sum_{k=1}^{K} h_k \sqrt{P_k} \mathbf{g}_k x_{k,(t)} b_k + \mathbf{n}_{(t)}, \ t = 1, \ldots, T, \quad (1)$$

where P_k is the transmit power of device k, h_k is the channel coefficient from device k to the BS, and $\mathbf{n}_{(t)} \sim \mathcal{CN}(\mathbf{0}, N_0\mathbf{I})$ is the background noise. Here, $b_k \in \{1, 0\}$ is the activity variable, which becomes 1 if device k becomes active and 0 otherwise. In addition, we assume that $\mathbb{E}[x_{k,(t)}] = 0$ and $\mathbb{E}[|x_{k,(t)}|^2] = 1$ for all k. Let

$$\mathbf{s}_{(t)} = [(h_1\sqrt{P_1}x_{1,(t)}b_1) \ \cdots \ (h_K\sqrt{P_K}x_{K,(t)}b_K)]^{\mathrm{T}}.$$

Then, $\mathbf{s}_{(t)}$ is a B-sparse vector where $B = \sum_{k=1}^{K} b_k$. The received signal can be re-written as

$$\mathbf{y}_{(t)} = \mathbf{G}\mathbf{s}_{(t)} + \mathbf{n}_{(t)}, \ t = 1, \ldots, T, \quad (2)$$

where $\mathbf{G} = [\mathbf{g}_1 \ \cdots \ \mathbf{g}_K] \in \mathbb{C}^{N \times K}$. In general, in order to support a number of devices, it is expected that $K \gg N$, which means conventional multiuser detectors (e.g., decorrelator detector) [34] cannot be used to directly estimate $\mathbf{s}_{(t)}$. However, since $\mathbf{s}_{(t)}$ is sparse provided that only a fraction of devices are being active at a time, the signal detection can be carried out by the device activity detection as in [15], [16] based on the notion of CS [12], [13]. That is, the support of $\mathbf{s}_{(t)}$ can be estimated, which provides the index set of active devices. If $B \le N$, any multiuser detector [34] can be used with known index set of active devices[1] to jointly detect the signals from active devices. Thus, it is important to have a reasonably good performance of the device activity detection (to estimate the index set of active devices) in grant-free CRA, and in this paper, we mainly focus on the device activity detection.

Noting that the support of $\mathbf{s}_{(t)}$ is the same for all $t \in \{1, \ldots, T\}$, the notion of MMV [25] [26] can be exploited for the device activity detection [35] [18] [23]. With a sufficiently large T and a sufficiently high receive signal-to-noise ratio (SNR), it is possible to detect up to $N - 1$ active devices. However, in practice, the receive SNR depends on fading and can be low. In addition, it is expected to keep the complexity of the receiver algorithm low. As a result, it might be difficult to detect up to $N - 1$ active devices.

In this paper, we apply the notion of NOMA to CRA to improve the performance without increasing system bandwidth or N. Throughout the paper, we assume that $\mathbf{g}_k$ is a realization of CSCG random vector, which is referred to as a Gaussian signature vector. In particular, $[\mathbf{g}_k]_n \sim \mathcal{CN}\left(0, \frac{1}{N}\right)$ is assumed. In addition, we assume that each device knows the channel coefficient (actually $|h_k|^2$), which is estimated using the beacon signal from the BS in time division duplexing (TDD) mode thanks to the channel reciprocity [3] [32]. Furthermore, the channel coefficients remain unchanged for a slot duration (i.e., the coherence time is longer than the slot duration).

III. LAYERED CRA APPROACH WITH SIC

In this section, we apply NOMA to CRA and discuss key parameters.

A. Application of NOMA to CRA

As in [32], we assume that there are Q different layers. Each layer is characterized by a different received signal power at the BS. In each layer, we assume that there are M devices with unique spreading codes and the resulting multiple access channels can be characterized in the two-dimensional domain as shown in Fig. 1 (a). An illustration of transmitted signals

---

[1]If the index set of active devices is known, we can have a submatrix of $\mathbf{G}$ by taking the columns corresponding to the active devices. In this case, the size of the submatrix of $\mathbf{G}$ becomes $N \times B$ and the corresponding system becomes underloaded, which means that a multiuser detector can be used to obtain a reliable estimate of the signals from B active devices [34].

for random access in the power and code domains is also illustrated in Fig. 1 (b). Throughout the paper, we assume that $K = QM$ (i.e., in each layer, there are $M = \frac{K}{Q}$ devices).
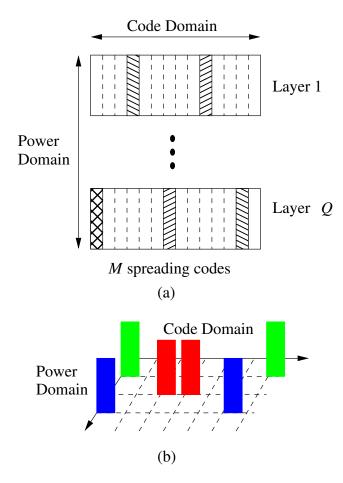

Fig. 1. The multiple access channels in the power and code domains: (a) 2-dimensional multiple access channels; (b) an illustration of transmitted signals for random access in the power and code domains.

Suppose that an active device, say device k, is in the qth layer. Then, the transmit power is decided to satisfy the following received power level:

$$P_k |h_k|^2 = V_q,$$

where V_q is the (pre-determined) received signal power for layer q. Note that if P_k is greater than the maximum transmit power due to deep fading, the device cannot be active (and needs to wait till the channel fading coefficient is sufficiently large). For convenience, let $V_1 > \ldots > V_Q \, (> 0)$. In addition, let $\mathbf{G}_q = [\mathbf{g}_{q,1} \; \ldots \; \mathbf{g}_{q,M}]$, where $\mathbf{g}_{q,m}$ represents the signature code for the mth device in layer q. Then, the received signal is re-written as

$$\mathbf{y}_{(t)} = \sum_{q=1}^{Q} \mathbf{G}_q \mathbf{s}_{q,(t)} + \mathbf{n}_{(t)}, \qquad (3)$$

where $[\mathbf{s}_{q,(t)}]_m = h_{q,m} \sqrt{P_{q,m}} x_{q,m,(t)} b_{q,m}$. Here, $h_{q,m}$, $P_{q,m}$, $x_{q,m,(t)}$, and $b_{q,m}$ are the channel coefficient, transmit power, data symbol, and activity variable of the mth device in layer q, respectively. The resulting approach is referred to as layered

NOMA-based random access [32], [36]. Note that the multiple access channels in layered NOMA-based random access in [32], [36] are orthogonal. However, in this paper, they are not orthogonal, because the spreading codes in each layer, i.e., $\mathbf{g}_{q,1}, \ldots, \mathbf{g}_{q,M}$, are not orthogonal to each other and $M > N$. Thus, in order to differentiate the resulting scheme from that in [32], [36], we call it layered CRA (L-CRA).

Note that due to non-orthogonal spreading codes with $M > N$, the determination of power levels is not straightforward and differs from that in [32]. We will discuss the determination of power levels in Section IV.

B. SIC and Limits of Recovery of Sparse Signals

In this subsection, we discuss SIC to decode the signals in each layer successively.

Let

$$\mathbf{y}_{q,(t)} = \mathbf{y}_{(t)} - \sum_{l=1}^{q-1} \mathbf{G}_l \mathbf{s}_{l,(t)} = \mathbf{G}_q \mathbf{s}_{q,(t)} + \mathbf{u}_{q,(t)}, \qquad (4)$$

where

$$\mathbf{u}_{q,(t)} = \sum_{l=q+1}^{Q} \mathbf{G}_l \mathbf{s}_{l,(t)} + \mathbf{n}_{(t)}.$$

Since $\mathbb{E}[x_{q,m,(t)}] = 0$, we have $\mathbb{E}[\mathbf{u}_{q,(t)}] = 0$. For convenience, let $\mathbb{E}[\mathbf{u}_{q,(t)} \mathbf{u}_{q,(t)}^{\mathrm{H}}] = \sigma_q^2 \mathbf{I}$, where the variance of the interference-plus-noise vector at layer q, σ_q^2, is to be discussed later. For convenience, define the SNR at layer q as

$$\mathrm{SNR}_q = \frac{V_q}{\sigma_q^2}.$$

In addition, let B_q and ρ_q be the number of active devices in layer q and the probability that a device in layer q becomes active, i.e., the access probability, respectively. Clearly, $\mathbb{E}[B_q] = M\rho_q$ as there are M devices in each layer. More importantly, we can see that σ_q^2 depends on $V_{q+1}, \ldots, V_Q$ as well as $\rho_{q+1}, \ldots, \rho_Q$.

In L-CRA, since there always exists the interference due to the signals in higher layers, the success of SIC depends on the background noise and interference (which also depends on the number of layers and power allocation). In general, for successful SIC for all layers with a high probability, it is necessary to carefully decide the power levels, $\{V_q\}$.

IV. DESIGN CRITERIA FOR SUCCESSFUL SIC WITH GAUSSIAN SPREADING

In L-CRA, as a power-domain NOMA scheme, the determination of power levels, $\{V_q\}$, is important to guarantee successful SIC with a high probability (which is required to avoid error propagation). In this section, we study design criteria for the power levels (when an optimal device activity detection approach is employed) through a large-system analysis under Gaussian approximations.

A. Gaussian Approximation for Interference

The interference vector in (4), i.e., $\mathbf{u}_{q,(t)}$, is Gaussian if $q = Q$ since $\mathbf{u}_{Q,(t)}$ only includes the background noise. For $q < Q$, since Gaussian spreading is considered (i.e., the signature vectors, $\{\mathbf{g}_{q,m}\}$, are Gaussian), $\mathbf{u}_{q,(t)}$ can be seen as a superposition of Gaussian vectors. Thus, for tractable analysis, we can consider the following assumption.

A0) $\mathbf{u}_{q,(t)}$ is a Gaussian random vector, i.e.,

$$\mathbf{u}_{q,(t)} \sim \mathcal{CN}(\mathbf{0}, \sigma_q^2 \mathbf{I}), \tag{5}$$

where

$$\sigma_q^2 = \sum_{l=q+1}^{Q} V_l M \rho_l + N_0. \tag{6}$$

In (6), $V_q M \rho_q$ is the variance of the signals in layer q.

In fact, the assumption of **A0** is an approximation, because the number of Gaussian signature vectors in each layer, i.e., B_q, is random. In other words, the sum of a random number of independent Gaussian random variables is not Gaussian as shown below.

Lemma 1. *Consider the sum of a random number of independent zero-mean Gaussian random variables as follows:*

$$Y = \sum_{k=1}^{B} X_k,$$

where $X_k \sim \mathcal{N}(0, \sigma^2)$ and B is a binomial random variable with parameters M and ρ. Let $Z \sim \mathcal{N}(0, M\rho\sigma^2)$ be a Gaussian random variable. Then, Y is subgaussian and, for positive integer k,

$$\mathbb{E}[Y^k] \geq \mathbb{E}[Z^k], \text{ for even } k > 2$$

and $\mathbb{E}[Y^k] = \mathbb{E}[Z^k] = 0$, for odd k, while $\mathbb{E}[Y^2] = \mathbb{E}[Z^2] = M\rho\sigma^2$.

Proof: The moment generating function (MGF) of Y can be found as

$$\mathbb{E}[e^{sY}] = (1 + \rho(\phi(s) - 1))^M,$$

where $\phi(s) = \mathbb{E}[e^{sX_k}] = e^{\frac{\sigma^2 s^2}{2}}$. Since $\phi(s) - 1 \geq 0$ for $s \in \mathbb{R}$, we can see that $(1 + \rho(\phi(s) - 1))^M$ increases with ρ. Thus,

$$(1 + \rho(\phi(s) - 1))^M \leq \phi(s)^M = e^{\frac{M\sigma^2 s^2}{2}},$$

which shows that Y is subgaussian.

Let $\mu_{m,k}$ denote the kth moment of the zero-mean Gaussian random variable with variance m. Since

$$\mu_{m,k} = \begin{cases} m^{k/2}(k-1)!!, & \text{if } k \text{ is even}, \\ 0, & \text{if } k \text{ is odd}, \end{cases} \tag{7}$$

we can show that

$$\begin{aligned} \mathbb{E}[Y^k] &= \sum_{m=0}^{M} p_m(M) \mathbb{E}[(X_1 + \ldots + X_m)^k] \\ &= \sum_{m=0}^{M} p_m(M) \sigma^k \mu_{m,k} \\ &= \begin{cases} \mathbb{E}[B^{\frac{k}{2}}] \sigma^k (k-1)!!, & \text{if } k \text{ is even}, \\ 0, & \text{if } k \text{ is odd}. \end{cases} \end{aligned} \tag{8}$$

where $\mathbb{E}[B^l] = \sum_{m=0}^{M} m^l p_m(M)$ and $p_m(M) = \binom{M}{m} \rho^m (1-\rho)^{M-m}$.

Let Z be the zero-mean Gaussian random variable with variance $M\rho\sigma^2$. Then, the moments of Z are given by [37]

$$\mathbb{E}[Z^k] = \begin{cases} (M\rho)^{k/2} \sigma^k (k-1)!!, & \text{if } k \text{ is even}, \\ 0, & \text{if } k \text{ is odd}. \end{cases} \tag{9}$$

From (8) and (9), the 2nd moments of Y and Z are the same, because $\mathbb{E}[B] = M\rho$. Furthermore, using Jensen's inequality, we have

$$\mathbb{E}\left[\left(\frac{B}{M\rho}\right)^l\right] \geq \left(\mathbb{E}\left[\frac{B}{M\rho}\right]\right)^l = 1, \ l \in \{0, 1, \ldots\},$$

which implies that $\mathbb{E}[B^l] \geq (M\rho)^l$. Applying this to (8) and (9), we can see that $\mathbb{E}[Y^k] \geq \mathbb{E}[Z^k]$ for all positive even integers k, which completes the proof. ∎

According to Lemma 1, since the moment of Y is higher than or equal to that of Z, we expect that the tail probability of Y is heavier than that of Gaussian Z. In Fig. 2, we show the probability distribution function (pdf) of Z and the histogram of Y when $\sigma^2 = 1$ and $M = 100$ and $\rho = 0.05$. Although the variances of Y and Z are the same, we can see that the tail probability of Y is heavier than that of Gaussian Z. However, since Y is subgaussian, the tail probability is also an exponential function.
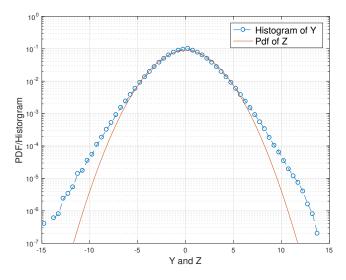

Fig. 2. The pdf and histogram of Z and Y, respectively, when $\sigma^2 = 1$ and $M = 100$ and $\rho = 0.05$.

In summary, although we consider the Gaussian approximation for $\mathbf{G}_q \mathbf{s}_{q,(t)}$ for tractable analysis, as shown above, it is expected that it results in an optimistic performance prediction.

B. An Optimal Approach for the Device Activity Detection under Gaussian Approximations

In this subsection, we consider an optimal approach for the device activity detection to derive design criteria. In particular, we consider the MAP approach [38].

Consider (4) under the assumption that the signals in layers $1, \ldots, q-1$ are perfectly recovered and removed. Let

$$\mathcal{I}_q = \text{supp}(\mathbf{s}_{q,(t)}), \ t = 1, \ldots, T.$$

The device activity detection is to detect (or estimate) $\mathcal{I}_q$ from $\mathbf{y}_q = [\mathbf{y}_{q,(1)}^{\mathrm{T}} \ \cdots \ \mathbf{y}_{q,(T)}^{\mathrm{T}}]^{\mathrm{T}}$. We note that

$$\mathbb{E}[|[\mathbf{s}_{q,(t)}]_k|^2] = \begin{cases} V_q, & \text{if } k \in \mathcal{I}_q \\ 0, & \text{o.w.} \end{cases}$$

Thus, we have the following assumption in order to derive a tractable approach for the device activity detection.

A1) For $k \in \mathcal{I}_q$, we assume that $[\mathbf{s}_{q,(t)}]_k$ is an independent zero-mean CSCG random variable with variance V_q, which is referred to as the Gaussian approximation [39] for the signal.

Under the Gaussian approximations for signal and interference (i.e., the assumptions of **A1** and **A0**, respectively), $\mathbf{y}_q$ becomes a Gaussian random vector with the following covariance matrix that depends on $\mathbf{b}_q = [b_{q,1} \ \cdots \ b_{q,M}]^{\mathrm{T}} \in \mathcal{B}$:

$$\mathbf{R}_q(\mathbf{b}_q) = \mathbf{G}_q \mathbf{B}_q \mathbf{G}_q^{\mathrm{H}} + \sigma_q^2 \mathbf{I},$$

where $\mathbf{B}_q = \mathrm{diag}(\mathbf{b}_q)$. Here, $\mathcal{B} = \{\mathbf{b} \,|\, [\mathbf{b}]_m \in \{0, 1\}\}$. As a result, the likelihood function of $\mathbf{b}_q$ for given $\mathbf{y}_q$ is given by

$$f(\mathbf{y}_q \,|\, \mathbf{b}_q) = \frac{\exp\left(-\sum_{t=1}^{T} \mathbf{y}_{q,(t)}^{\mathrm{H}} \mathbf{R}_q(\mathbf{b}_q)^{-1} \mathbf{y}_{q,(t)}\right)}{\pi^N \det(\mathbf{R}_q(\mathbf{b}_q))}. \quad (10)$$

Since the a posteriori probability is given by

$$\Pr(\mathbf{b}_q \,|\, \mathbf{y}_q) = C f(\mathbf{y}_q \,|\, \mathbf{b}_q) \Pr(\mathbf{b}_q),$$

where C is a constant, the MAP approach for the device activity detection can be given by

$$\begin{aligned} \hat{\mathbf{b}}_q &= \underset{\mathbf{b}_q \in \mathcal{B}}{\mathrm{argmax}} \, \Pr(\mathbf{b}_q \,|\, \mathbf{y}_q) \\ &= \underset{\mathbf{b}_q \in \mathcal{B}}{\mathrm{argmax}} \, \ln f(\mathbf{y}_q \,|\, \mathbf{b}_q) + \ln \Pr(\mathbf{b}_q). \end{aligned} \quad (11)$$

Throughout the paper, we assume that each device becomes independently active. Thus, we have the following assumption.

A2) $\Pr(\mathbf{b}_q)$ can be represented by a binomial distribution as follows:

$$\Pr(\mathbf{b}_q) = \prod_{m=1}^{M} \Pr(b_{q,m}) = \binom{M}{B_q} \rho_q^{B_q} (1 - \rho_q)^{M - B_q}, \quad (12)$$

where ρ_q is the probability of being active for the devices in layer q and $B_q = ||\mathbf{b}_q||_0$.

Since $\mathbf{b}_q$ is a binary vector of length M, the computational complexity of the MAP approach is proportional to $|\mathcal{B}| = 2^M$, which might be prohibitively high when there are a large number of devices (as $M = K/Q$), although it is to be used to derive design criteria (in Subsection IV-C). To avoid this problem, we will consider a low-complexity approach in Section V.

C. A Large-System Analysis

For convenience, we omit the layer index q. Denote by $\mathbf{b}$ the true activity vector. Consider two vectors $\mathbf{b}, \mathbf{b}' \in \mathcal{B}$, where $\mathbf{b} \neq \mathbf{b}'$. Let $\mathbf{y} = [\mathbf{y}_{(1)}^{\mathrm{H}} \ \cdots \ \mathbf{y}_{(T)}^{\mathrm{H}}]^{\mathrm{H}}$ and

$$\mathcal{L}_{\mathrm{ap}}(\mathbf{b}) = \mathcal{L}(\mathbf{b}) + \ln \Pr(\mathbf{b}),$$

where $\mathcal{L}(\mathbf{b}) = \ln f(\mathbf{y} \,|\, \mathbf{b})$.

When the MAP detection is considered, from (11), the pairwise error probability (PEP) [40] is given by

$$\begin{aligned} P(\mathbf{b} \to \mathbf{b}') &= \Pr(\mathcal{L}_{\mathrm{ap}}(\mathbf{b}) < \mathcal{L}_{\mathrm{ap}}(\mathbf{b}') \,|\, \mathbf{b}) \\ &= \Pr\left(\sum_t \mathbf{y}_{(t)}^{\mathrm{H}} \mathbf{\Delta} \mathbf{y}_{(t)} > d(\mathbf{b}, \mathbf{b}') \,|\, \mathbf{b}\right), \quad (13) \end{aligned}$$

where $\mathbf{\Delta} = \mathbf{R}(\mathbf{b})^{-1} - \mathbf{R}(\mathbf{b}')^{-1}$ and

$$\begin{aligned} d(\mathbf{b}, \mathbf{b}') &= \ln \Pr(\mathbf{b}) - \ln \Pr(\mathbf{b}') \\ &\quad - T(\ln \det(\mathbf{R}(\mathbf{b})) - \ln \det(\mathbf{R}(\mathbf{b}'))). \quad (14) \end{aligned}$$

We can have a useful representation of $\sum_t \mathbf{y}_{(t)}^{\mathrm{H}} \mathbf{\Delta} \mathbf{y}_{(t)}$ to find the PEP for certain cases as follows.

Lemma 2. *Let $\mathbf{e} = \mathbf{b}' - \mathbf{b}$ and suppose that $\mathrm{supp}(\mathbf{e}) = l$ (i.e., $\mathbf{b}$ differs from $\mathbf{b}'$ by only one element). Then, under the assumption of **A1**, for given $\mathbf{b}$, we have*

$$\sum_{t=1}^{T} \mathbf{y}_{(t)}^{\mathrm{H}} \mathbf{\Delta} \mathbf{y}_{(t)} = \begin{cases} \frac{1}{2} \frac{V \alpha_l}{1 + V \alpha_l} \chi_{2T}^2 \ (\geq 0), & \text{if } e_l = 1; \\ -\frac{1}{2} V \alpha_l' \chi_{2T}^2 \ (\leq 0), & \text{if } e_l = -1, \end{cases} \quad (15)$$

where χ_n^2 represents a chi-squared random variable with n degrees of freedom and

$$\alpha_l = \mathbf{g}_l^{\mathrm{H}} \mathbf{A}(\mathbf{b}) \mathbf{g}_l \ \text{ and } \ \alpha_l' = \mathbf{g}_l^{\mathrm{H}} \mathbf{A}(\mathbf{b}') \mathbf{g}_l. \quad (16)$$

Here, $\mathbf{A}(\mathbf{b}) = \mathbf{R}(\mathbf{b})^{-1}$.

Proof: See the proof of Lemma 3 in [41]. ∎

The case of $e_l = +1$ corresponds to the event of false alarm (FA) where device l is not active, but the receiver decides that it is active, while that of $e_l = -1$ corresponds to the event of missed detection (MD) where device l is active, but the receiver does not see it. Thus, in Lemma 2, we only consider the event of one MD or one FA. Although there can be the events of more than one MDs or FAs or mixed MDs and FAs, their probabilities might be sufficiently low to ignore, compared to that of the event of one MD or one FA.

As derived in [41], when $\mathrm{supp}(\mathbf{e}) = e_l = +1$, we can show that

$$\begin{aligned} d(\mathbf{b}, \mathbf{b}') &= d_{\mathrm{FA}}(||\mathbf{b}||_0) \\ &= T \ln(1 + V \alpha_l) + \ln \frac{||\mathbf{b}||_0 + 1}{M - ||\mathbf{b}||_0} + \ln \frac{1 - \rho}{\rho}. \end{aligned}$$

In addition, when $e_l = -1$, it follows

$$d(\mathbf{b}, \mathbf{b}') = -d_{\mathrm{MD}}(||\mathbf{b}||_0),$$

where

$$d_{\mathrm{MD}}(||\mathbf{b}||_0) = T \ln(1 + V \alpha_l') - \ln \frac{M - ||\mathbf{b}||_0 + 1}{||\mathbf{b}||_0} - \ln \frac{\rho}{1 - \rho}.$$

Thus, by substituting (15) into (13), the PEPs of FA and MD are given by

$$\begin{aligned} \mathbb{P}_{\mathrm{FA}}(||\mathbf{b}||_0) &= \Pr\left(\chi_{2T}^2 > \frac{2 d_{\mathrm{FA}}(||\mathbf{b}||_0)}{\xi_l}\right) \\ \mathbb{P}_{\mathrm{MD}}(||\mathbf{b}||_0) &= \Pr\left(\chi_{2T}^2 < \frac{2 d_{\mathrm{MD}}(||\mathbf{b}||_0)}{V \alpha_l'}\right), \quad (17) \end{aligned}$$

where $\xi_l = \frac{\alpha_l}{1 + \alpha_l}$.

We now consider a large-system with $N \to \infty$ [42]. Since $||\mathbf{b}||_0$ is the number of active devices, as in [42], we assume that $\frac{||\mathbf{b}||_0}{N}$ approaches a constant as follows:

$$\frac{||\mathbf{b}||_0}{N} \to \kappa = \frac{\rho M}{N}, \ N \to \infty.$$

From (16), it can be shown that

$$\alpha_l = \gamma \mathbf{g}_l^{\mathrm{H}} \left(\mathbf{I} + \gamma \tilde{\mathbf{G}} \tilde{\mathbf{G}}^{\mathrm{H}} \right)^{-1} \mathbf{g}_l, \tag{18}$$

where $\tilde{\mathbf{G}}$ is the submatrix of $\mathbf{G}$ with the columns corresponding to the support of $\mathbf{b}$ and $\gamma = \frac{1}{\sigma^2}$. According to [42], α_l can be seen as the signal-to-interference ratio (SIR) of the minimum mean-squared error (MMSE) receiver. When the elements of $\mathbf{g}_l$ are independent and identically distributed (i.i.d.) and $\mathbf{g}_l$ and $\tilde{\mathbf{G}}$ are independent, for approximation, we can use the mean of α_l (where the expectation is carried out over the elements of $\mathbf{g}_l$ and $\tilde{\mathbf{G}}$) that is given by

$$\alpha_l \approx \mathbb{E}[\alpha_l] = \beta(\gamma, ||\mathbf{b}||_0/N),$$

where $\beta(\cdot, \cdot)$ is derived in [42] as follows:

$$\beta(\gamma, \kappa) = \frac{(1-\kappa)\gamma}{2} - \frac{1}{2} + \sqrt{\frac{(1-\kappa)^2\gamma^2}{4} + \frac{(1+\kappa)\gamma}{2} + \frac{1}{4}}. \tag{19}$$

We can also replace α_l' with its mean for approximation to find $\mathbb{P}_{\mathrm{MD}}$ as follows:

$$\alpha_l' \approx \mathbb{E}[\alpha_l'] = \beta(\gamma, ||\mathbf{b}'||_0/N).$$

Since $\frac{||\mathbf{b}||_0}{N}, \frac{||\mathbf{b}'||_0}{N} \to \kappa$ as $N \to \infty$, we have

$$\alpha_l, \alpha_l' \to \beta(\gamma, \kappa) \tag{20}$$

in a large-system. Furthermore, we have

$$\ln \frac{||\mathbf{b}||_0 + 1}{M - ||\mathbf{b}||_0} \to \ln \frac{\rho}{1-\rho}$$
$$\ln \frac{M - ||\mathbf{b}||_0 + 1}{||\mathbf{b}||_0} \to \ln \frac{1-\rho}{\rho}. \tag{21}$$

Consequently, in a large-system, we have

$$\frac{d_{\mathrm{FA}}(||\mathbf{b}||_0)}{T\xi_l} \to \frac{(1+\beta)\ln(1+V\beta)}{\beta}$$
$$\frac{d_{\mathrm{MD}}(||\mathbf{b}||_0)}{TV\alpha_l'} \to \frac{\ln(1+V\beta)}{V\beta}, \tag{22}$$

where $\beta = \beta(\gamma, \kappa)$. The asymptotic probabilities of (one) FA and (one) MD become

$$\tilde{\mathbb{P}}_{\mathrm{FA}} = \Pr\left(\frac{\chi_{2T}^2}{2T} > \frac{(1+\beta)\ln(1+V\beta)}{\beta} \right)$$
$$\tilde{\mathbb{P}}_{\mathrm{MD}} = \Pr\left(\frac{\chi_{2T}^2}{2T} < \frac{\ln(1+V\beta)}{V\beta} \right). \tag{23}$$

In (23), since we have $\mathbb{E}\left[\frac{\chi_{2T}^2}{2T} \right] = 1$, low error probabilities are expected for a sufficiently large T if

$$\frac{(1+\beta)\ln(1+V\beta)}{\beta} > 1$$
$$\frac{\ln(1+V\beta)}{V\beta} < 1. \tag{24}$$

According to [43], for example, we can have the following bound:

$$\tilde{\mathbb{P}}_{\mathrm{MD}} \leq \exp\left(-\frac{T}{2}\left(1 - \frac{\ln(1+V\beta)}{V\beta} \right) \right).$$

Thus, if the conditions in (24) hold, $\tilde{\mathbb{P}}_{\mathrm{MD}}$ can exponentially decrease with T (which is also valid $\tilde{\mathbb{P}}_{\mathrm{FA}}$) in a large-system. We can have the following result to determine V.

Lemma 3. *If*

$$V\beta > 1 \text{ and } V \geq 1, \tag{25}$$

(24) *holds.*

Proof: Since

$$\frac{x}{1+x} \leq \ln(1+x) \leq x, \ x > -1, \tag{26}$$

we can show that

$$\frac{(1+\beta)\ln(1+V\beta)}{\beta} \geq \frac{(1+\beta)V\beta}{\beta(1+V\beta)} = \frac{V(1+\beta)}{1+V\beta} > 1,$$

which shows that the first inequality in (24) holds. To show the second inequality, we can apply the second in equality in (26), which completes the proof. ∎

D. Determination of Power Levels

In this subsection, we consider a cell and discuss an approach to determine the power levels according to the conditions in (25).

As shown in Fig. 3, suppose that a cell is divided into Q regions. Region q is a circular ring with the inner and outer radii, denoted by R_{q-1} and R_q, respectively, where $R_0 = 0$. Thus, the transmit power of a device in region q needs to be higher than that in region $q - 1$ for the same receive power. Thus, in order to avoid a high transmit power, the devices in region q can be assigned to layer q [32].

Suppose that K devices are uniformly distributed in a cell. Then, $\{R_q\}$ can be decided to make the area of each region equal (so that each area has the same number of devices (on average), $M = \frac{K}{Q}$). For normalization purposes, we assume that $R_1 = 1$. Since the power control is considered for the pre-determined receive power levels, for a device in region or layer q, we expect

$$P_{q,m} \propto R_q^\eta V_q,$$

where η is the path loss exponent. Here, we consider a device on the outer ring (i.e., the worst case) and $|h_k|^2 \propto \frac{1}{R_q^\eta}$.
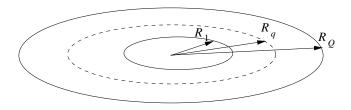

Fig. 3. An illustration of dividing a cell into Q regions to reduce the transmit power.

With a target SNR, denoted by Γ, for given access probabilities, $\{\rho_q\}$, the power levels can be recursively decided as follows:

$$V_q = \frac{\Gamma}{\beta\left(\frac{1}{\sigma_q^2}, \kappa\right)}, \ q = Q, \ldots, 1. \tag{27}$$

Here, for $q = Q$, since $V_Q = \frac{\Gamma}{\beta\left(\frac{1}{N_0}, \kappa\right)}$, we need to have

$$\Gamma \geq \beta\left(\frac{1}{N_0}, \kappa\right) \tag{28}$$

to make sure that $V_Q \geq 1$. Note that since $\beta(\gamma, \kappa)$ increases with γ and $\sigma_q^2 > \sigma_{q+1}^2$, from (27), we can see that $V_1 > \ldots > V_Q$ as expected.

For example, suppose that $Q = 3$, $M = 100$, $N = 30$, and $\rho_q = 0.05$ for all q. Then, there might be 15 active devices on average. In addition, let $\Gamma = 4$, $\eta = 3.5$, and $N_0 = 1$. In Table I, the pre-determined power levels, $\{V_q\}$, and the average transmit powers for three layers are shown, where we can see that by taking advantage of shorter distances to the BS, the transmit power of the devices in region q can be lower than V_q for $q < Q$.

TABLE I
THE TRANSMIT POWER FOR EACH REGION AND THE PRE-DETERMINED
POWER LEVEL FOR EACH LAYER.

Layer	R_q	V_q (dB)	Transmit Power (dB)
1	0.577	32.840	24.490
2	0.816	19.618	16.536
3	1	6.382	6.382

In this section, although we only consider the determination of power levels to satisfy (24), it might be possible to jointly determine the power levels and access probabilities. We also note that the average transmit power of the devices in layer 1 might be too high although the advantage of the short distance to the BS in layer 1 is taken into account when $Q = 3$ as shown in Table I. Thus, Q may not be too large to avoid a high transmit power (e.g., we may have L-CRA with two layers in practice).

V. VARIATIONAL INFERENCE BASED LOW-COMPLEXITY DETECTION

For the device activity detection, we use any low-complexity CS algorithm that can exploit the sparse activity as in [16] [20] [22] [18] [23]. However, in Subsection IV-B, since the MAP approach is considered for the design criteria, it might be desirable to consider the MAP detector. Unfortunately, its complexity is prohibitively high as mentioned earlier and we need to resort to low-complexity approximations. In this section, we consider a variational inference technique, namely the coordinate ascent variational inference (CAVI) algorithm [44], [45], which can provide a low-complexity approximate solution to the MAP detection problem in (11).

For convenience, we omit the layer index q. In (11), the activity variables, which are binary random variables, are to be detected. If an exhaustive search is considered, the complexity is proportional to $|\mathcal{B}| = 2^M$ for each layer. To avoid this, we

can consider the variational distribution for each b_m, denoted by $\psi_m(b_m)$, and solve the following optimization problem:

$$\psi^*(\mathbf{b}) = \underset{\psi(\mathbf{b}) \in \Psi}{\operatorname{argmin}} \, \mathrm{KL}(\psi(\mathbf{b}) \| \Pr(\mathbf{b} \,|\, \mathbf{y})), \tag{29}$$

where $\psi(\mathbf{b}) = \prod_m \psi(b_m)$, Ψ represents the collection of all the possible distributions of $\mathbf{b}$, and $\mathrm{KL}(\cdot)$ is the Kullback-Leibler (KL) divergence that is defined as

$$\mathrm{KL}(\psi(\mathbf{b}) \| f(\mathbf{b})) = \sum_{\mathbf{b}} \psi(\mathbf{b}) \ln \frac{\psi(\mathbf{b})}{f(\mathbf{b})}.$$

Here, $f(\mathbf{b})$ is any distribution of $\mathbf{b}$ with $f(\mathbf{b}) > 0$ for all $\mathbf{b} \in \mathcal{B}$. In (29), clearly, we attempt to find $\psi(\mathbf{b})$ that is close to the a posteriori probability, $\Pr(\mathbf{b} \,|\, \mathbf{y})$, as an approximation. In [45], the minimization of the KL divergence is equivalent to the maximization of the evidence lower bound (ELBO), which is given by

$$\mathrm{ELBO}(\psi) = \mathbb{E}[\ln f(\mathbf{y}, \mathbf{b})] - \mathbb{E}[\ln \psi(\mathbf{b})].$$

Let $\mathbf{b}_{-m} = [b_1 \ \ldots \ b_{m-1} \ b_{m+1} \ \ldots \ b_M]^{\mathrm{T}}$ and $\psi_{-m}(\mathbf{b}_{-m}) = \sum_{l \neq m} \psi_l(b_l)$. The CAVI algorithm [44], [45] is to update one variational distribution at a time with the other variational distributions fixed (so that the ELBO can be minimized through iterations) as follows:

$$\begin{aligned} \psi_m^*(b_m) &\propto \theta_m(b_m) \\ &= \exp\left(\mathbb{E}_{-m}[\ln f(b_m \,|\, \mathbf{b}_{-m}, \mathbf{y})]\right), \end{aligned} \tag{30}$$

where $\mathbb{E}_{-m}[\cdot]$ represents the expectation with respect to $\mathbf{b}_{-m}$ or with the distribution $\psi_{-m}(\mathbf{b}_{-m})$. Let $\psi_m^{(i)}$ denote the ith estimate of ψ_m. In the CAVI algorithm, $\psi_m^{(i)}$ is updated from $m = 1$ to M in each iteration. The number of iterations is denoted by N_{run}. Unfortunately, the convergence behavior of the CAVI algorithm is not known [45] and N_{run} can be decided through experiments.

Thanks to the Gaussian approximations, it is possible to find a closed-form expression for $\theta_m(b_m)$ in (30), which can be found in [46], where it is also shown that the complexity of the CAVI algorithm per iteration is $O(MN^2)$.

VI. SIMULATION RESULTS

In this section, we present simulation results for L-CRA. We assume that a cell is divided into Q regions and the devices in region q can perform the power control so that the received powers at the BS become V_q. In addition, the power levels are decided as in (27) with $\eta = 3.5$ and $N_0 = 1$, and in each simulation run, Gaussian spreading codes are randomly generated.

For the device activity detection at the BS, we use the CAVI algorithm. To see the performance, we consider the numbers of MD and FA devices, where an MD device is an active device that is not detected and an FA device is an inactive device that is detected (as an active device). Throughout this section, for convenience, we assume that the BS knows the number of active devices in each layer, B_q, and carry out the device activity detection by choosing the devices associated with the B_q largest $\psi_m(1)$'s in each layer. In this case, the number of MD devices and that of FA devices are the same. Note

that in L-CRA with $Q > 1$, there is error propagation due to erroneous SIC in the presence of FA as well as MA devices. Thus, the presence of either FA or MD devices degrades the performance, while MD devices can lead a worse performance degradation than FA devices (in terms of the throughput[2]), because MD devices need to re-transmit their packets.

Before we see the impact of key system parameters (e.g., access probability ρ, target SNR Γ, and spreading gain N) on the performance, we consider the number of iterations of the CAVI algorit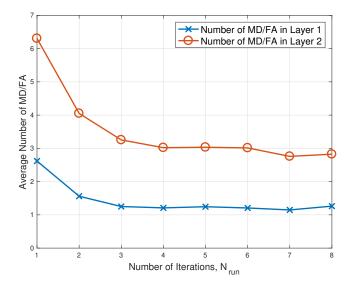hm to see the convergence. In Fig. 4, we show the average number of MD/FA devices as a function of the number of iterations for CAVI, N_{run}, when $Q = 2$, $M = 150$, $N = 30$, $\rho = 0.05$, $\Gamma = 4$, and $T = 100$. Clearly, as expected, a better performance is achieved with more iterations. However, we can see that $N_{\text{run}} \geq 4$ might be sufficient as the performance improvement becomes negligible with increasing N_{run} once $N_{\text{run}} \geq 4$.

Fig. 4. The average number of MD/FA devices as a function of the number of iterations for CAVI, N_{run}, when $Q = 2$, $M = 150$, $N = 30$, $\rho = 0.05$, $\Gamma = 4$, and $T = 100$.

We now consider the performance of L-CRA depending on the system parameters with $N_{\text{run}} = 5$ for the CAVI algorithm. In particular, in order to see the advantage of applying NOMA to CRA, let us consider the performances with $Q = 1, 2, 3$ when there are $K = 300$ devices. Fig. 5 (a) shows the average total number of MD/FA devices as a function of the access probability, $\rho = \rho_q$, for all q, when $N = 30$, $\Gamma = 4$, $T = 100$, and $N_{\text{run}} = 5$. We can see that the average total number of MD/FA devices decreases with Q. When ρ is sufficiently low (e.g., $\rho < 0.05$), the average total number of MD/FA devices with $Q = 3$ is sufficiently small (e.g., less than 2). In particular, in the case of $\rho = 0.04$ (where the average total number of active devices is 12), the average total numbers of MD/FA devices are 6.71, 1.90, and 0.66 when $Q = 1$, 2, and 3, respectively. Thus, the error rate decreases by a factor of about 3.53 or 10.16 from conventional CRA (i.e., $Q = 1$) to

[2]Note that in this paper, we do not consider the throughput as no re-transmission strategies are considered

L-CRA with $Q = 2$ or 3, respectively. However, as mentioned earlier, the transmit power at devices increases with Q, which might be the cost of a better performance.

In Fig. 5 (b), the average number of MD/FA devices in each layer is shown when $Q = 3$. It is clearly shown that there is the error propagation as the average number of MD/FA devices increases with q. However, although the error propagation exists, as shown in Fig. 5 (a), a better performance can be achieved with a larger Q. As expected, the average number of MD/FA devices increases with the access probability, ρ. Note that when $\rho = 0.1$, the average number of active devices per layer is 10. Thus, when $Q = 3$, according to Fig. 5 (b), most active devices in layer 3 are incorrectly detected (i.e., about 8 out of 10). On the other hand, if $\rho = 0.05$, the average number of MD/FA devices is approximately 1 in layer 3, which means that approximately 20% of the active devices in layer 3 are incorrectly detected. This implies that the access probability should be low enough to avoid excessive re-transmissions.

In the rest of the section, we only consider the case of $Q = 2$ as the transmit power of the devices in layer 1 might be too high when $Q = 3$ (which is more than 24dB) as shown in Table I. Note that if $Q = 2$, the average transmit power of the devices in layer 1 becomes 16.221dB under the same conditions in Table I.

To see the impact of the spreading gain, N, on the performance, the average number of MD/FA devices is shown as a function of the spreading gain, N, in Fig. 6 when $Q = 2$, $M = 150$, $\rho = 0.05$, $\Gamma = 4$, $T = 100$, and $N_{\text{run}} = 5$. Clearly, the number of MD/FA devices decreases with N. Thus, for a lower probability of incorrect detection, we need a wider system bandwidth.

Fig. 7 shows the average number of MD/FA devices as a function of the target SNR, Γ, when $Q = 2$, $M = 150$, $N = 30$, $\rho \in \{0.025, 0.05\}$, $T = 100$, and $N_{\text{run}}) = 5$. The average number of MD/FA devices decreases with Γ until Γ reaches 9dB. However, as Γ further increases from 9dB, the average number of MD/FA devices increases. This indicates that a too high target SNR does not help improve the performance. When the signals in layer 1 are detected, the superposition of the signals in layer 2 becomes the dominant term in the interference-plus-noise, $\mathbf{u}_{1,(t)}$, for a high Γ. As explained in Subsection IV-A, the superposition of the signals in layer 2 is not exactly Gaussian and has a tail probability that is heavier than that of Gaussian. This results in a higher error probability. Note that at a high target SNR (say $\Gamma = 16$dB), the performance degradation when $\rho = 0.025$ is less severe than that when $\rho = 0.05$. This is due to the fact that the background noise becomes more dominant than the interference with a lower ρ, which leads to a relatively lower tail probability and less performance degradation. In general, it is desirable to avoid a high target SNR, which is also preferable in terms of keeping the transmit power of devices low.

VII. CONCLUDING REMARKS

In this paper, we have applied power-domain NOMA to CRA, which results in L-CRA, to improve the performance of CRA without increasing the system bandwidth. While
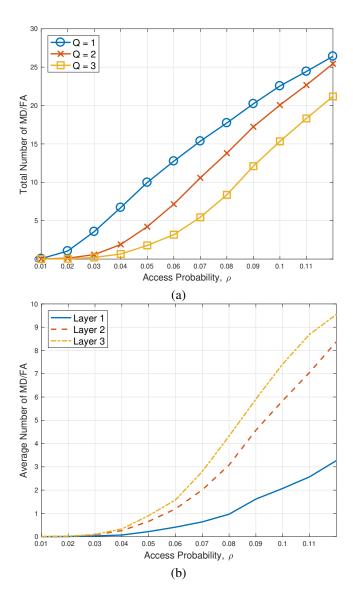
(a)

(b)

Fig. 5. The average number of MD/FA devices as a function of access probability when $K = 300$, $N = 30$, $\Gamma = 4$, $T = 100$, and $N_{\mathrm{run}} = 5$: (a) the total number of MD/FA devices with $Q \in \{1, 2, 3\}$; (b) the number of MD/FA devices for each layer with $Q = 3$.

Fig. 6. The average number of MD/FA devices as a function of the spreading gain, N, when $Q = 2$, $M = 150$, $\rho = 0.05$, $\Gamma = 4$, $T = 100$, and $N_{\mathrm{run}} = 5$.

Fig. 7. The average number of MD/FA devices as a function of the target SNR, Γ, when $Q = 2$, $M = 150$, $N = 30$, $\rho \in \{0.025, 0.05\}$, $T = 100$, and $N_{\mathrm{run}} = 5$.

the application of NOMA to CRA was straightforward, the main issue was the determination of the power levels for multiple layers in the power domain to allow successful user activity detection with a high probability. Through a large-system analysis with Gaussian spreading, we derived design criteria to determine the power levels. Since the MAP detection was used in deriving the design criteria, a low-complexity detection method that provides approximate MAP solution was presented using a variational inference approach, namely the CAVI algorithm. Simulation results showed that the error rate of the device activity detection can decrease by a factor of about 3.53 or 10.16 from conventional CRA to L-CRA with two or three layers, respectively, with a low access probability, which demonstrates that L-CRA could have a higher throughput or support more devices than conventional CRA.
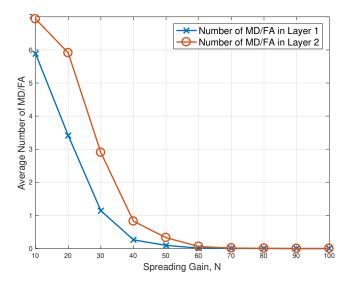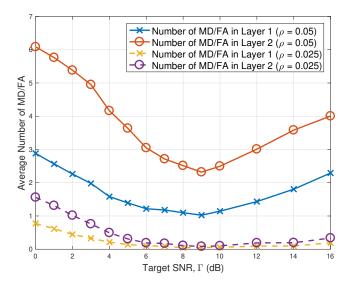
REFERENCES

[1] M. Condoluci, M. Dohler, G. Araniti, A. Molinaro, and K. Zheng, "Toward 5G densenets: architectural advances for effective machine-type communications over femtocells," *IEEE Communications Magazine*, vol. 53, pp. 134–141, January 2015.

[2] H. Shariatmadari, R. Ratasuk, S. Iraji, A. Laya, T. Taleb, R. Jntti, and A. Ghosh, "Machine-type communications: current status and future perspectives toward 5G systems," *IEEE Communications Magazine*, vol. 53, pp. 10–17, September 2015.

[3] C. Bockelmann, N. Pratas, H. Nikopour, K. Au, T. Svensson, C. Stefanovic, P. Popovski, and A. Dekorsy, "Massive machine-type communications in 5G: physical and MAC-layer solutions," *IEEE Communications Magazine*, vol. 54, pp. 59–65, September 2016.

[4] T. Taleb and A. Kunz, "Machine type communications in 3GPP networks: potential, challenges, and solutions," *IEEE Communications Magazine*, vol. 50, pp. 178–184, March 2012.

[5] 3GPP TR 37.868 V11.0, *Study on RAN improvments for machine-type communications*, October 2011.

[6] 3GPP TS 36.321 V13.2.0, *Evolved Universal Terrestrial Radio Access (E-UTRA); Medium Access Control (MAC) protocol specification*, June 2016.

[7] N. Abramson, "THE ALOHA SYSTEM: Another alternative for computer communications," in *Proceedings of the November 17-19, 1970, Fall Joint Computer Conference*, AFIPS '70 (Fall), (New York, NY, USA), pp. 281–285, ACM, 1970.

[8] O. Arouk and A. Ksentini, "Multi-channel slotted aloha optimization for machine-type-communication," in *Proc. of the 17th ACM International Conference on Modeling, Analysis and Simulation of Wireless and Mobile Systems*, pp. 119–125, 2014.

[9] T. M. Lin, C. H. Lee, J. P. Cheng, and W. T. Chen, "PRADA: Prioritized random access with dynamic access barring for MTC in 3GPP LTE-A networks," *IEEE Trans. Vehicular Technology*, vol. 63, pp. 2467–2472, Jun 2014.

[10] C. H. Chang and R. Y. Chang, "Design and analysis of multichannel slotted ALOHA for machine-to-machine communication," in *Proc. IEEE GLOBECOM*, pp. 1–6, Dec 2015.

[11] J. Choi, "On the adaptive determination of the number of preambles in RACH for MTC," *IEEE Communications Letters*, vol. 20, pp. 1385–1388, July 2016.

[12] D. Donoho, "Compressed sensing," *IEEE Trans. Information Theory*, vol. 52, pp. 1289–1306, April 2006.

[13] E. Candes, J. Romberg, and T. Tao, "Robust uncertainty principles: exact signal reconstruction from highly incomplete frequency information," *IEEE Trans. Information Theory*, vol. 52, pp. 489–509, Feb 2006.

[14] G. Wunder, P. Jung, and C. Wang, "Compressive random access for post-LTE systems," in *Proc. IEEE ICC*, pp. 539–544, June 2014.

[15] H. Zhu and G. Giannakis, "Exploiting sparse user activity in multiuser detection," *IEEE Trans. Communications*, vol. 59, pp. 454–465, February 2011.

[16] L. Applebaum, W. U. Bajwa, M. F. Duarte, and R. Calderbank, "Asynchronous code-division random access using convex optimization," *Physical Communication*, vol. 5, no. 2, pp. 129–147, 2012.

[17] H. F. Schepker, C. Bockelmann, and A. Dekorsy, "Exploiting sparsity in channel and data estimation for sporadic multi-user communication," in *Proc. ISWCS 2013*, pp. 1–5, Aug 2013.

[18] J. Choi, "Stability and throughput of random access with CS-based MUD for MTC," *IEEE Trans. Vehicular Technology*, vol. 67, pp. 2607–2616, March 2018.

[19] Y. D. Beyene, R. Jantti, and K. Ruttik, "Random access scheme for sporadic users in 5G," *IEEE Trans. Wireless Communications*, vol. 16, pp. 1823–1833, March 2017.

[20] H. F. Schepker, C. Bockelmann, and A. Dekorsy, "Efficient detectors for joint compressed sensing detection and channel decoding," *IEEE Trans. Communications*, vol. 63, pp. 2249–2260, June 2015.

[21] J. Choi, "Two-stage multiple access for many devices of unique identifications over frequency-selective fading channels," *IEEE Internet of Things J.*, vol. 4, pp. 162–171, Feb 2017.

[22] G. Wunder, I. Roth, R. Fritschek, and J. Eisert, "Performance of hierarchical sparse detectors for massive MTC," 2018.

[23] L. Liu, E. G. Larsson, W. Yu, P. Popovski, C. Stefanovic, and E. de Carvalho, "Sparse signal processing for grant-free massive connectivity: A future paradigm for random access protocols in the Internet of Things," *IEEE Signal Processing Magazine*, vol. 35, pp. 88–99, Sept 2018.

[24] J. Choi, "Compressive random access with coded sparse identification vectors for MTC," *IEEE Trans. Communications*, vol. 66, pp. 819–829, Feb 2018.

[25] J. Chen and X. Huo, "Theoretical results on sparse representations of multiple-measurement vectors," *IEEE Trans. Signal Processing*, vol. 54, pp. 4634–4643, Dec 2006.

[26] M. E. Davies and Y. C. Eldar, "Rank awareness in joint sparse recovery," *IEEE Trans. Information Theory*, vol. 58, pp. 1135–1146, Feb 2012.

[27] J. Choi, "Non-orthogonal multiple access in downlink coordinated two-point systems," *IEEE Commun. Letters*, vol. 18, pp. 313–316, Feb. 2014.

[28] Z. Ding, Z. Yang, P. Fan, and H. Poor, "On the performance of non-orthogonal multiple access in 5G systems with randomly deployed users," *IEEE Signal Process. Letters*, vol. 21, pp. 1501–1505, Dec 2014.

[29] K. Higuchi and A. Benjebbour, "Non-orthogonal multiple access (NOMA) with successive interference cancellation for future radio access," *IEICE Trans. Commun.*, vol. E98.B, no. 3, pp. 403–414, 2015.

[30] Z. Ding, Y. Liu, J. Choi, M. Elkashlan, C. L. I, and H. V. Poor, "Application of non-orthogonal multiple access in LTE and 5G networks," *IEEE Communications Magazine*, vol. 55, pp. 185–191, February 2017.

[31] Y. Liang, X. Li, J. Zhang, and Z. Ding, "Non-orthogonal random access for 5G networks," *IEEE Trans. Wireless Communications*, vol. 16, pp. 4817–4831, July 2017.

[32] J. Choi, "NOMA based random access with multichannel ALOHA," *IEEE J. Selected Areas in Communications*, vol. 35, pp. 2736–2743, Dec 2017.

[33] J. Choi, *Adaptive and Iterative Signal Processing in Communications*. Cambridge University Press, 2006.

[34] S. Verdu, *Multiuser Detection*. Cambridge University Press, 1998.

[35] J. Choi, "On the stability and throughput of compressive random access in MTC," in *2017 IEEE International Conference on Communications (ICC)*, pp. 1–6, May 2017.

[36] J. Choi, "Layered non-orthogonal random access with SIC and transmit diversity for reliable transmissions," *IEEE Trans. Communications*, vol. 66, pp. 1262–1272, March 2018.

[37] A. Papoulis and S. U. Pillai, *Probability, Random Variables and Stochastic Processes*. McGraw-Hill, fourth ed., 2002.

[38] J. Choi, *Optimal Combining and Detection*. Cambridge University Press, 2010.

[39] C. Lin, W. Wu, and C. Liu, "Low-complexity ML detectors for generalized spatial modulation systems," *IEEE Trans. Communications*, vol. 63, pp. 4214–4230, Nov 2015.

[40] E. Biglieri, *Coding for Wireless Channels*. New York: Springer, 2005.

[41] J. Choi, "MCMC based detection for random access with preambles in MTC," *IEEE Trans. Communications*, pp. 1–1, 2018.

[42] D. N. C. Tse and S. V. Hanly, "Linear multiuser receivers: effective interference, effective bandwidth and user capacity," *IEEE Trans. Information Theory*, vol. 45, pp. 641–657, Mar 1999.

[43] B. Laurent and P. Massart, "Adaptive estimation of a quadratic functional by model selection," *Ann. Statist.*, vol. 28, pp. 1302–1338, 10 2000.

[44] C. M. Bishop, *Pattern Recognition and Machine Learning (Information Science and Statistics)*. Berlin, Heidelberg: Springer-Verlag, 2006.

[45] D. M. Blei, A. Kucukelbir, and J. D. McAuliffe, "Variational inference: A review for statisticians," *Journal of the American Statistical Association*, vol. 112, no. 518, pp. 859–877, 2017.

[46] J. Choi, "A Variational Inference based Detection Method for Repetition Coded Generalized Spatial Modulation," *IEEE Trans. Communications*, (to be published).